

Conversion of C5 into C6 Cyclic Species through the Formation of C7 Intermediates[†]

Carlo Cavallotti,* Silvia Mancarella, Renato Rota, and Sergio Carrà

Dip. Chimica, Materiali e Ingegneria Chimica "G. Natta"/CIIRCO, Politecnico di Milano, Via Mancinelli 7, 20131 Milano, Italy

Received: October 30, 2006; In Final Form: January 10, 2007

We have recently proposed that the addition of C₂H₂ to the cyclopentadienyl radical can lead to the rapid formation of the cycloheptatrienyl radical and, in succession, of the indenyl radical. These reactions represent an interesting and unexplored route for the enlargement of gas-phase cyclic species. In this work we report *ab initio* calculations we performed with the aim of investigating in detail the gas-phase reactivity of cycloheptatrienyl and indenyl radicals. We found that the reaction of the cycloheptatrienyl radical with atomic hydrogen can lead to its fast conversion into the more stable benzyl radical. This reaction pathway involves the intermediate formation of heptatriene, norcaradiene, and toluene. Successively we investigated whether this reaction mechanism can be extended to polycyclic aromatic hydrocarbons (PAHs). For this purpose we studied the reaction of C₂H₂ with the indenyl radical, which can be considered as a superior homologue of the cyclopentadienyl radical. This reaction proceeds through a pathway similar to that proposed for C₅H₅ but with a reaction rate about an order of magnitude smaller. The present calculations extend thus the previously proposed C5–C7–C9 mechanism to bicyclic PAH and suggest a fast route for the conversion of C5 into C6 cyclic radicals, mediated by the formation of C7 cyclic species.

1. Introduction

A large part of the hazardous health of atmospheric pollution, which is related for instance to lung cancer and cardiopulmonary disease,¹ is probably due to fine soot particles arising from incomplete fuels combustion, since they can be deeply breathed into the lungs. This adverse effect of soot particles might be also related to their association with polycyclic aromatic hydrocarbons (PAHs), some of which are mutagenic.² Consequently, in the last years a large attention has been paid to the emissions of PAHs and soot from combustion processes,³ also in consideration of the fact that combustion will still represent, at least for the next decades, the main source of power.

The reduction of PAHs and soot formation in combustion processes requires a better physical and chemical understanding of the chemical processes responsible for their formation and growth. Although many important details on PAHs and soot formation and growth are not yet completely understood, there is a general agreement on the main features of the processes involved, as reviewed for instance by Richter and Howard⁴ and Frenklach.⁵ These processes start with the formation of molecular precursors of the soot (that is, PAHs with molecular weight equal to 500–1000 amu) through addition of small molecules and cyclization followed by the soot inception from heavy PAHs and by the growth of soot particles through addition of gaseous molecules or reactive particle–particle collisions.

This means that reactions involved in the formation of small cyclic hydrocarbons have a key role in the chemical reaction pathways responsible for PAH and soot growth. In this framework, it is clear the importance of fundamental studies aimed at elucidating different reaction channels leading to small PAH. Several pathways have been proposed in literature, as

reviewed for instance by Lindstedt.⁶ Among the others, it is worthwhile mentioning the important patterns involving HACA-type sequences,⁷ propargyl radicals recombination,⁸ acetylene reaction with C4 radicals,⁵ as well as cyclopentadienyl radical recombination.⁹

Of particular interest are the reactions involving the cyclopentadienyl radical (cC₅H₅). This is a chemical species characterized by a significant thermodynamic stability, which makes it one of the most abundant radical species observed in combustion environments. Since thermodynamic stability is usually related to a lack of reactivity, bimolecular reactions involving cC₅H₅ as a reactant can usually proceed at a significant rate only having as a reacting partner another radical species. This is for example the case of the reaction pathway proposed by Melius et al.,⁹ according to which two cC₅H₅ radicals can react to form naphthalene and thus transform a biradical system composed of two 5-membered rings in a larger molecule comprising two C6 ring.

In a recent work we have investigated computationally the reactions that follow the addition of C₂H₂ to cC₅H₅.¹⁰ This reaction is of some interest since both C₂H₂ and cC₅H₅ are often present in high concentrations in flames. We found that this reaction can proceed quickly leading to the formation of the cycloheptatrienyl radical (cC₇H₇) through the reaction mechanism reported in Scheme 1.

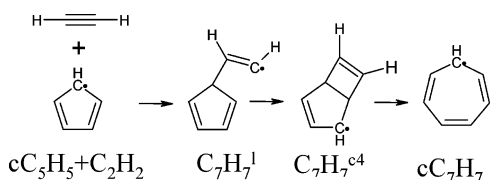
This reaction pathway was found to be the fastest of three different mechanisms we examined and the only one in quantitative agreement with experimental evidence, reported in the literature, according to which cC₅H₅ can react fast in the gas phase to form an undetermined C₇H₇ species.¹¹ Our calculations lead us to believe that the measured C₇H₇ signal could be attributed to the cycloheptatrienyl radical, cC₇H₇.

To get some more insight into the reactivity of cC₇H₇, of which not much is known, we investigated theoretically some reaction pathways of cC₇H₇. One that was found to proceed at a significant rate is sketched in Scheme 2. The kinetic constants

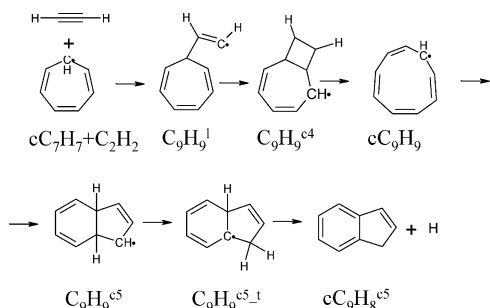
[†] Part of the special issue "James A. Miller Festschrift".

* To whom correspondence should be addressed. E-mail: carlo.cavallotti@polimi.it. Phone: ++39-02-23993176. Fax: ++39-02-23993180.

SCHEME 1: Kinetic Pathway Proposed To Describe the Reactivity Originated by the Addition of Acetylene to cC_5H_5 in Which the Cycloheptatrienyl Radical Appears as the Product



SCHEME 2: Kinetic Mechanism Proposed To Describe the Reactivity Originated by the Addition of Acetylene to cC_7H_7



for the overall reactions $cC_5H_5 + C_2H_2 \rightarrow cC_7H_7$ and $cC_7H_7 + C_2H_2 \rightarrow cC_9H_8 + H$ were determined using quantum Rice–Ramsperger–Kassel (QRRK) theory at atmospheric pressure as $2.2 \times 10^{11} \exp(-6440/T(K))$ and $6.6 \times 10^{11} \exp(-10\,080/T(K)) \text{ cm}^3 \text{ mol}^{-1} \text{ s}^{-1}$, respectively. The corresponding backward kinetic constants were $4.2 \times 10^{16} T^{-1} \exp(-30\,850/T(K)) \text{ s}^{-1}$ and $4.2 \times 10^{14} \exp(-27\,300/T(K)) \text{ cm}^3 \text{ mol}^{-1} \text{ s}^{-1}$, respectively.¹⁰ It is here interesting to observe that as much as the kinetic pathway reported in Scheme 1 provides a route that can lead to the enlargement of cC_5H_5 rings on the other side the backward reaction is fast enough that, in the absence of an alternative reaction pathway, it would lead to the decomposition of cC_7H_7 at high rates at sufficiently high temperatures. A possible reaction pathway for cC_7H_7 is its conversion to the more stable benzyl radical. This is an interesting possibility since it has been recently proposed that the pyrolysis of benzyl can lead to the formation of cC_5H_5 and C_2H_2 .¹² Thus, if a sufficiently fast mechanism of conversion of cC_7H_7 into benzyl exists, then the C5–C7 mechanism we propose might be an intermediate step of the benzyl decomposition mechanism. However, other authors^{12,13} who studied the same reaction have proposed that benzyl decomposes to an indeterminate C_7H_6 species and hydrogen, which only successively might react to form other species, such as cC_5H_5 and C_2H_2 . Also, in our previous work¹⁰ we have calculated that benzyl and cC_7H_7 are separated by an activation energy higher (~ 90 kcal/mol) than that experimentally measured for the decomposition of benzyl (~ 80 kcal/mol). The potential energy surface (PES) of C_7H_7 has been theoretically investigated by Jones et al. with the aim of identifying possible decomposition pathways of the benzyl radical.¹⁴ The computed activation energies for the several kinetic pathways investigated were however significantly larger than those experimentally measured, which indicates that further work is required to understand this system.

In this framework, the first part of this work is devoted to improving our understanding of the cC_7H_7 reactivity and in particular to study its possible conversion into the benzyl radical. In fact, despite the high thermodynamic stability of cC_7H_7 , it is possible that at high temperatures a significant part of it

dissociates back to cC_5H_5 and C_2H_2 , rather than react to form cC_9H_8 through the reaction pathway sketched in Scheme 2. However cC_7H_7 can also follow other reaction paths rather than those constituted by the addition of C_2H_2 or the decomposition in cC_5H_5 and C_2H_2 ; among these, the reaction with atomic hydrogen, usually present in high concentrations in fuel-rich combustion environments, to give cycloheptatriene (CHT). Such a species involves a very rich chemistry, as it can exist in at least four different isomers that at relatively low temperatures can be interconverted one into the other. In particular 1,3,5-cycloheptatriene can thermally isomerize to form bicyclo[4.1.0]-hepta-2,4-diene (norcardiene), bicyclo[2.2.1]hepta-2,4-diene (norbornadiene), and eventually toluene, which is the most thermodynamically stable isomer. The kinetics of the thermal C_7H_8 isomerization has been extensively investigated both experimentally^{15,16} and theoretically.^{17,18} It was found that the internal rearrangements are determined by ring opening and closure reactions and by hydrogen transposition reactions. Once toluene is formed, it can decompose into the benzyl and phenyl radicals. The possible conversion of cC_7H_7 into benzyl is of great interest since benzyl is considered in many reaction mechanisms a key species for explaining PAHs and soot formation, which can be formed mainly through its reactions with acetylene and propargyl radicals.^{19,20}

In the second part of this work we have investigated along the same lines the reactivity of species larger than cC_5H_5 , such as the indenyl radical reactions to give fluorene. The aim was to determine whether the previous reaction mechanisms have a generality that transcends the specificity of the reactions previously investigated and can be therefore considered as a viable mechanism for describing the reactivity of gas-phase species having C5 rings stabilized by highly delocalized radicals.

2. Method and Theoretical Background

The reaction mechanisms here investigated are characterized by the succession of several unimolecular isomerization reactions started by a bimolecular exothermic addition involving at least one radical among the reactants. As a consequence, the reaction intermediates are characterized by being in a vibrationally excited state, which description requires the use of a suitable kinetic theory. The best candidate would be Rice–Ramsperger–Kassel–Marcus (RRKM) theory, which, used in conjunction with the solution of the master equation, would allow to describe correctly the flow across the PES of the excited complexes. However RRKM requires much information on the PES and several approximations are often taken in the formulation of the master equation in order to solve it efficiently. Moreover all the reactions here considered are characterized by PESs with multiple potential energy wells, which makes the system rather complicated. Thus, since in this work we were mainly interested in investigating the feasibility of a possible reaction mechanism rather than determining with extreme precision the value of a particular kinetic constant, we preferred to use QRRK to calculate overall rate constants. To improve the counting of the density of states of the activated intermediates involved in the considered reaction mechanisms and to relax the constraints associated with the use of a single mean vibrational frequency for each molecule to evaluate the microcanonical reaction rate, we modified QRRK theory. On the whole, our work relies on the QRRK theory formulation proposed by Dean,²¹ modified so that two vibrational frequencies, rather than one, are used to determine microcanonical reaction probabilities and the chemical activation distribution function. The extension of QRRK from the use of one to two

mean vibrational frequencies has the advantage, over the recently proposed extension of the same theory to three mean vibrational frequencies,²² to maintain the possibility to have a straightforward analytic formulation. In particular, if we assume that the excess vibrational energy should be distributed between two frequencies, ν_1 and ν_2 , each S_1 and S_2 times degenerate, with $S_1 + S_2$ equal to the total number of oscillators $S_{\text{tot}} = 3N_{\text{atoms}} - 6$, then the population of the activated state at energy N with respect to the fundamental state can be expressed as

$$K(N,T) = \sum_{J=1}^N \alpha_1^J \alpha_2^K (1 - \alpha_1)^{S_1} (1 - \alpha_2)^{S_2} \frac{(J + S_1 - 1)! (K + S_2 - 1)!}{J!(S_1 - 1)! K!(S_2 - 1)!} \quad (1)$$

where J are the quanta of energy in the S_1 oscillators, K is equal to $(N - J)\nu_2/\nu_1$ and represents the quanta of energy in the S_2 oscillators, and α_i is equal to $\exp(-h\nu_i/k_bT)$. The chemical activation distribution function can then be computed as suggested by Dean²¹ as

$$f(N,T) = \frac{k_{-1}(N,T)K(N,T)}{\sum_{N=N_{\text{crit}}}^{\infty} k_{-1}(N,T)K(N,T)} \quad (2)$$

where k_{-1} is the microcanonical rate of dissociation of the excited state to reactants. The chemical activation distribution function multiplied by the kinetic constant of the reaction of formation of the first adduct and by the concentration of reactants gives the rate of formation of the adduct at energy E , with $E = h\nu_i N$. The concentration of each adduct can then be calculated imposing the pseudo-steady-state approximation on its formation rate, as long as the microcanonical rate coefficients of each reaction channel are known. This approach, which allows to avoid solving the master equation to determine the population of each state of energy E , is strictly valid only when intermediate adducts excited at different energies are in Boltzmann equilibrium. This is probably the strongest approximation in the present treatment of internal energy transfer and can be removed only by solving directly the master equation. We will comment further this point in the result section.

The microcanonical rate coefficients for each reaction channel can then be computed as

$$k_i(N,T) = A_i \sum_{J=m}^{\infty} \frac{(J - m + S_1 - 1)! (K + S_2 - 1)!}{(J - m)!(S_1 - 1)! K!(S_2 - 1)!} \sum_{J=0}^{\infty} \frac{(J + S_1 - 1)! (K + S_2 - 1)!}{J!(S_1 - 1)! K!(S_2 - 1)!} \quad (3)$$

where J and K are the same as those defined in eq 1, m is the number of energy quanta equal to the activation energy, and A_i is the reaction pre-exponential factor, which we assume to be equal to that defined in transition state theory. One of the advantages of the formulation of microcanonical rate constants in this form is that if the frequency of the first harmonic oscillator is chosen as equal to that of the bond that is being broken in the reaction, then the evaluation of the probability of having enough energy in that specific oscillator to let the reaction proceed is more accurate than that provided by single-frequency QRRK theory. This is also consistent with the removal of one vibrational degree of freedom from the counting of the density of states in the transition state that is at the basis of the

formulation of both transition state theory and RRKM. The consistency between the present formulation of QRRK and RRKM can be further improved imposing that the vibrational partition function that can be calculated through the ensemble of two families of oscillators, each populated S_1 and S_2 times, is equal to the complete vibrational partition function

$$\left(\frac{1}{1 - \exp(-h\nu_1/k_bT)} \right)^{S_1} \left(\frac{1}{1 - \exp(-h\nu_2/k_bT)} \right)^{S_2} = \prod_{i=1}^{S_{\text{tot}}} \frac{1}{1 - \exp(-h\nu_i/k_bT)} \quad (4)$$

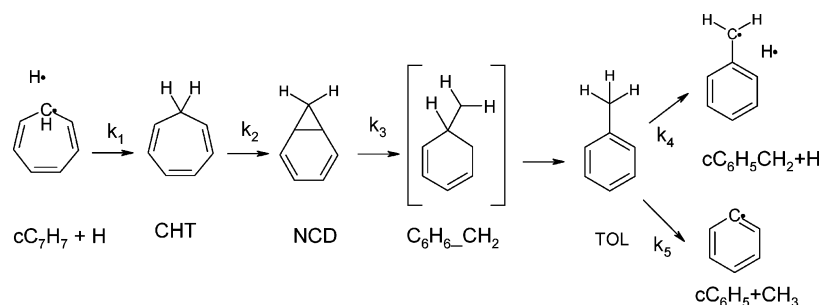
Since $S_1 + S_2$ is equal to S_{tot} , this equation is a function of only one variable, S_1 , and it can be solved at each temperature once the adduct vibrational frequencies are known. The only degrees of freedom that remain to be saturated to solve eqs 1–4 are thus the values of the vibrational frequencies. In general, we assigned to one vibrational frequency the value of the stretching frequency of the bond that is being broken, while for the other a low value is usually adopted, in order to decrease the spacing between the different energy states and thus improve their counting. Usually values lower than 800 cm^{-1} leads to converged microcanonical rate coefficients.

Vibrational frequencies of reactants, excited states, and products were computed with density functional theory in the harmonic approximation at the B3LYP/6-31+g(d,p) level. The loss of energy due to collisions with the bath gas was modeled using the modified strong collision approach proposed by Troe.^{23,24} The total collision rate was calculated as the Lennard-Jones collision frequency for energy transfer, which was expressed as

$$Z_{\text{LJ}} = \frac{P}{RT} \pi \sigma_{\text{AB}}^2 \sqrt{\frac{8k_bT}{\pi \mu_{\text{AB}}}} \Omega_{\text{AB}}^{(2,2)*} \quad (5)$$

with the collision integral calculated as suggested by Troe. The collisional stabilization rate constant was finally determined multiplying eq 5 by the collision efficiencies parameter β suggested by Troe.²⁴ Calculations were performed assuming a N_2 bath gas with a mean energy transferred per collision of 382 cal/mol, which was experimentally measured for the deactivation of excited toluene.²⁵

Kinetic constants of each elementary reaction involved in the kinetic mechanism were determined using conventional transition state theory. Structures of reactants, transition states, and products were computed using density functional theory at the B3LYP/6-31+g(d,p) level. Energies were evaluated at a higher level of theory using the hybrid G2MP2 approach on structures optimized at the B3LYP/6-31+g(d,p) level. This approach gives energies in better agreement with experimental data than the standard G2MP2 approach and is usually referred to as B3-G2MP2. In particular we found that we could calculate energies in better agreement with experimental data if we did not include the high level correction suggested for G2MP2 theory.²⁶ This is probably due to the high accuracy of geometries calculated with density functional theory. All electronic energies were corrected with zero point energies (ZPE) calculated at the B3LYP/6-31+g(d,p) level. The ZPE correction was not scaled. Kinetic constants were corrected for quantum tunneling using the Wigner approximation. All transition states were characterized by possessing a single imaginary vibrational frequency and, when appropriate, were determined using the synchronous transit guided method using as guess structures calculated performing

SCHEME 3: Kinetic Pathway Proposed for the Conversion of the Cycloheptatrienyl into the Benzyl Radical^a

^a The reaction is started by atomic hydrogen addition, and $\text{C}_6\text{H}_6\text{-CH}_2$ is an intermediate state.

a scan of the PES as a function of the reaction coordinate. All quantum mechanical calculations were performed with the G03 program suite.²⁷

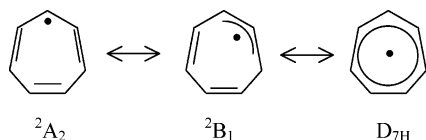
The rates of reactions proceeding without passing from a distinct transition state were computed using variational transition state theory (VTST). This in particular was the case for all the hydrogen addition/dissociation reactions. The potential energy surface used in VTST calculations was computed using an unrestricted wave function at the UB3LYP/6-31+g(d,p) level. A similar approach was successfully adopted by Tokmakov et al. to calculate the rate of decomposition of cyclopentadiene in the cyclopentadienyl radical and atomic hydrogen.²⁸

3. Reaction between Atomic Hydrogen and the Cycloheptatrienyl Radical

Because of its internal symmetry, resonance stabilization, and gas-phase thermodynamic stability, the cycloheptatrienyl radical is very similar to the cyclopentadienyl radical. Since they differ in chemical composition only by a C_2H_2 group, it is likely that, if there is a fast reaction pathway between acetylene and cC_5H_5 that can lead to the formation cC_7H_7 , then a significant amount of it will be formed in any generic combustion environment. As discussed in the introduction, we have shown that such a fast reaction pathway actually exists, and it is only slightly activated, so that the reaction of formation of cC_7H_7 can proceed fast also at moderate temperatures. However, the presence of the cycloheptatrienyl radical has scarcely been observed or proposed to explain particular reaction pathways in flames. This can be due either to the difficulty of distinguishing this chemical species from its more stable isomer, the benzyl radical, or to the fact that at high temperature a fast pathway might exist to convert cC_7H_7 in benzyl, so that once cC_7H_7 is produced it is also rapidly consumed. While the investigation of the cC_7H_7 PES has shown that the isomerization of cC_7H_7 to benzyl is likely to be hindered by an activation energy significantly higher than that necessary to decompose it to cC_5H_5 and C_2H_2 , it is known that the isomerization of CHT to toluene is relatively slightly activated. The activation energy for this reaction has in fact been computed and experimentally measured to be about 52 kcal/mol.^{16,18} Thus, since the addition of hydrogen to cC_7H_7 leads to the formation of CHT, which can then isomerize to toluene and eventually decompose in benzyl and atomic hydrogen, we decided to investigate this reaction pathway, as it represents a possible cC_7H_7 –benzyl conversion pathway. The reaction mechanism we propose is based on the heptatriene–toluene reaction pathway proposed by Jarzecki¹⁷ and is sketched in Scheme 3. According to this mechanism, the addition of atomic hydrogen to cC_7H_7 leads to the formation of CHT, which can then either dissociate back to reactants, or cyclize to form norbornadiene (NCD). NCD can follow two reaction pathways: the first is the reverse reaction and leads back to CHT, while

the other involves the opening of the strained C3 ring and the formation of an activated state, $\text{cC}_6\text{H}_6\text{-CH}_2$. A transposition of a hydrogen atom will then lead to the formation of toluene. According to the CASSCF study of Jarzecki et al.,¹⁷ the transition from NCD to toluene involves the change of the molecular spin from singlet to triplet and the formation of a symmetric intermediate species, $\text{cC}_6\text{H}_6\text{-CH}_2$, in which a hydrogen is bound to the same carbon atom, sp^3 hybridized, to which is bound the CH_2 group. Thus the search of the reaction transition state of this reaction involves accounting for spin inversion. Recently, Klippenstein et al. investigated the same PES with the aim of studying the decomposition of toluene in benzyl and phenyl radicals.¹⁸ They adopted an unrestricted wave function to locate the transition state that characterizes the transition from NCD to toluene and performed calculations at the UB3LYP/6-31g(d) level. The activation energy for this reaction was successively calculated at the CCSD(T) level using a correlation consistent cc-pvdz basis set. To reproduce the experimental reaction rate of the $\text{TOL} \rightarrow \text{CHT}$ reaction the computed activation energy had to be increased by 2 kcal/mol.¹⁸ In this work we searched the PES of the $\text{NCD} \rightarrow \text{TOL}$ reaction at the B3LYP/6-31+G(d,p) level using a restricted wave function. The PES was studied as a function of three reaction coordinates, the first of which was one of the two C–C bonds by which the CH_2 group of NCD is bound to the C6 cycle. The other two were respectively the distance between the migrating hydrogen atom and the C atom of the C6 ring to which it is bound in the reactant state and the distance between the same atom and the C atom of the CH_2 group. The saddle point determining the transition state was found imposing that the force constants of all the reaction coordinates are smaller than 0.01 and was characterized through a frequency calculation by possessing a single imaginary vibrational frequency. The transition state wave function is unstable with respect to modifications. In particular the energy of the triplet is slightly higher than that of the restricted singlet, while the unrestricted singlet energy is the lowest. However force constants calculated with the unrestricted wave function are smaller than the 0.01 thresholds we imposed as criteria for locating the transition state. This indicates that transition state structures determined with restricted and unrestricted DFT singlet wave functions are similar.

Similarly to what was found by Jarzecki et al.,¹⁷ the reaction initially proceeds through the stretching of one of the two C–C bonds of the CH_2 group and the formation of a symmetric intermediate in which the C atom of the CH_2 group lies on the symmetry axis of the C6 ring. However, differently from what was found in the previous work, this intermediate is a singlet and unstable with respect to regression to the NCD geometry. Successively the reaction proceeds through the transposition of the hydrogen atom, positioned on the sp^3 C of the C6 ring, to

SCHEME 4: Bonding in Three Possible Electronic States for the cC_7H_7 Radical


the CH_2 group to form toluene. The activation energy for this reaction is 46.8 kcal/mol, about three kcal/mol higher than that calculated by Klippenstein et al.,¹⁸ and thus similar to the value they used to match experimental data.

The kinetic constant for the reaction between hydrogen and the CHT radical was calculated as the backward kinetic constant imposing the thermodynamic consistence. This procedure, which is standard in the evaluation of kinetic constants of reactions proceeding without passing from a distinct transition state, is complicated by the fact that the cycloheptatrienyl radical is distorted by its symmetric structure by a significant Jahn–Teller effect. The same Jahn–Teller distortion affects the cC_5H_5 radical, whose effect on its thermodynamic properties was deeply investigated theoretically in several works.^{28–30} It was shown that cC_5H_5 is distorted from the expected D_{5h} symmetry to two C_{2v} ground states, 2A_2 and 2B_1 , of nearly identical energies. The slight energy difference between this two resonance structures can result in a fast and unhindered motion of the C atoms of the C_5 ring and thus in a substantial increase of the entropy of this molecule. Also C_7H_7 is distorted from the D_{7h} symmetry to give two C_{2v} ground states, 2A_2 and 2B_1 . The bonding in the different electronic states is sketched in Scheme 4. The correct evaluation of the entropy of this molecule requires determining a specific PES for the nuclear motion, formulating an appropriate Schrödinger equation, and then calculating a Jahn–Teller partition function. An alternative approach, which was found valid at a first level of approximation, was to calculate the molecular entropy using vibrational frequencies and rotational symmetry of the D_{7h} symmetry, while the electronic energy can be determined using one of the two C_{2v} structures.²⁹ In particular Ikeda et al. calculated a cC_5H_5 entropy value in good agreement with the more refined theoretical estimates using D_{5h} frequencies and replacing the lowest vibrational frequency with a one-dimensional rotational partition function with a fictitious inertia moment.³¹ In the present work, we evaluated the cC_7H_7 entropy using a rotational symmetry number of 14, vibrational frequencies calculated in the D_{7h} symmetry, and an electronic degeneracy of 2. As expected, the electronic energy of the D_{7h} structure is significantly higher than that of the two C_{2v} structures, because of the Jahn–Teller distortion. Thus relative energies on the C_7H_8 PES were calculated using as reference for cC_7H_7 its 2A_2 structure, whose energy is similar to that of the 2B_1 structure.

The rate of the reaction of hydrogen dissociation from CHT was determined using VTST on a PES determined at the UB3LYP/6-31+g(d,p) level. The PES was computed for a C–H distance varying between 2.0 and 4.0 Å at intervals of 0.1 Å. Similarly to what found by Tokmakov et al.²⁸ for the cC_5H_6 PES, the reaction enthalpy change calculated at the B3LYP/6-31+g(d,p) level, 66 kcal/mol, is smaller than that determined at the B3-G2MP2 level. In particular we calculated a hydrogen binding energy of 74.3 kcal/mol, using the following isodesmic reaction: $cC_5H_5 + cC_7H_8 \rightarrow cC_5H_6 + cC_7H_7$, where we used as reference value for the hydrogen binding energy in cyclopentadiene the 82.5 kcal/mol value suggested by Tokmakov.²⁸ The PES used in the VTST calculations was thus rescaled to match the isodesmic limit and is sketched in Figure 1. As it

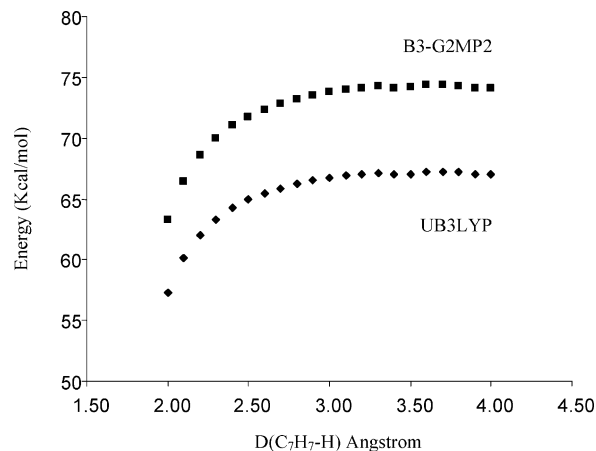


Figure 1. cC_7H_7 –H dissociation PES computed at the UB3LYP/6-31+g(d,p) level and rescaled at the B3-G2MP2 isodesmic enthalpy change value. The latter was used in the VTST calculations.

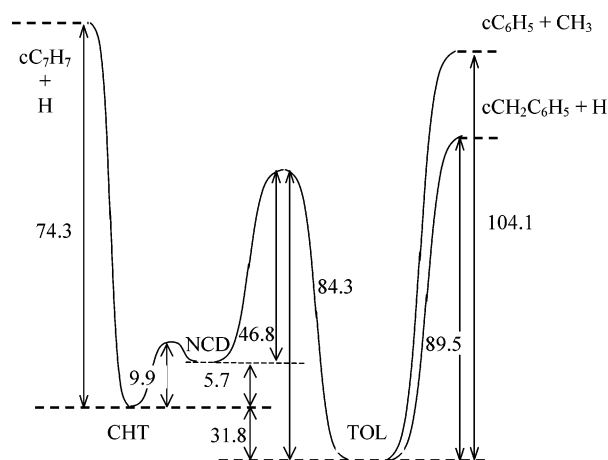


Figure 2. PES of the $H + cC_7H_7$ reaction. All energies were calculated at the B3-G2MP2 level and corrected with ZPE and are reported in kcal/mol.

can be observed, DFT and B3-G2MP2 energies differ by several kcal/mol. This is in part due to the relatively small size of the basis set used in the DFT calculations and in part to the inadequacy of DFT in treating this system. This is the reason why we systematically calculated energies, when the number of atoms to be considered made it possible, using a higher level ab initio theory such as B3-G2MP2, which includes a systematic correction for the size of the basis set. The reliability of this approach for a similar system is confirmed by the good agreement between the cC_5H_5 –H bond energy calculated at the B3-G2MP2 level of theory, 80.9 kcal/mol, and the recommended data (82.5 kcal/mol).²⁸

Activation energies and enthalpy changes, calculated at the G2MP2 level on structures optimized at the B3LYP/6-31+g(d,p) level, are reported in Figure 2. Calculated kinetic constants of elementary reactions determined using conventional transition state theory and fitted in the 1000–2500 K temperature range are reported in Table 1. The kinetic constants of the reactions of decomposition of toluene in the benzyl and phenyl radicals were taken from the literature.¹⁸

Overall kinetic constants for the investigated reaction mechanism were calculated using the two-frequency version of QRRK theory described in the method section. Possible products of the reaction considered in the calculations were CHT, NCD, toluene, all produced through collisional stabilization, and the benzyl and phenyl radicals. The two frequencies used in the calculations to calculate the chemical activation distribution

TABLE 1: TST Kinetic Constants for the Reaction Mechanism That Follows the Addition of H to cC₇H₇ Fitted between 1000 and 2500 K^a

reaction	A_{forw}	α	$E_{a(\text{forw})}$	A_{back}	α	$E_{a(\text{back})}$
cC ₇ H ₇ + H → CHT	3.2×10^{13}	0.250	0.03	3.0×10^{18}	-0.902	78.0
CHT → NCD	8.9×10^9	0.901	9.2	1.3×10^{10}	0.969	3.8
NCD → toluene	4.6×10^{12}	0.646	48.0	5.5×10^{12}	0.423	87.4
toluene → benzyl + H	1.6×10^{13}	0.682	89.2			
toluene → phenyl + CH ₃	4.3×10^{22}	-1.733	104.2			

^a Kinetic parameters are reported in units consistent with kcal, s, mol, and cm in the form $k = AT^\alpha \exp(-E_a/RT)$. Energies calculated at the B3-G2MP2 level as described in the text, except for the last two reactions, which kinetic constants were taken from the literature (see ref 18).

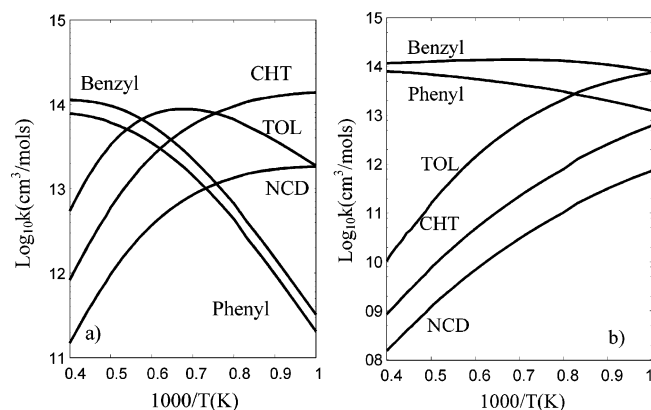


Figure 3. Results of bifrequency QRRK calculations performed at atmospheric (a) and reduced (101 Pa) (b) pressure for the reaction between H and cC₇H₇.

function and the energy dependent rate constants were 3000 and 500 cm⁻¹. The first value was chosen as it corresponds to the stretching vibrational frequency of the dissociating hydrogen in toluene, while for the second we used a low value in order to decrease the energetic step size adopted in the calculation of the microcanonical rate constants. The results of the calculations are reported in Figure 3 at two different pressures.

The calculated QRRK rates indicate that CHT and the benzyl radical are the major products of the reaction at low and high temperatures, respectively. Phenyl is also among the main products of the reaction at high temperatures, with a rate constant about a factor of 2 smaller than that of the benzyl channel. This is similar to the C₆H₅/(C₆H₅+C₇H₇) branching ratio calculated by Klippenstein et al.¹⁸ using RRKM/master equation for the toluene decomposition reaction. Similar calculations performed using the standard single frequency QRRK theory predicted, on the contrary, that phenyl is produced at a higher rate than benzyl, which is indicative of the limits of this theory. It is also important to remark that the reaction rate for the dissociation of the excited complex back to reactants is smaller than the reaction rates sketched in Figure 3 at all temperatures, which indicates that the reaction between H and cC₇H₇ is extremely effective. Moreover, since the rate of conversion of CHT into toluene is much higher than that of dissociation to cC₇H₇ and H, as the activation energy of the first process is at least 20 kcal/mol smaller than that of the second, we can conclude that, at all temperatures, the reaction between cC₇H₇ and H will eventually result in the formation of a C₆ cyclic species, which can be toluene or the benzyl radical depending on the temperature and pressure. The interpolated kinetic constant between 1000 and 2500 K for the reaction cC₇H₇ + H → benzyl/phenyl + H/CH₃ are $2.2 \times 10^{63}T^{-13.01} \exp(-29\,509/T(\text{K}))$ and $1.2 \times 10^{61}T^{-12.43} \exp(-28\,682/T(\text{K}))$ at atmospheric pressure and $1.3 \times 10^{25}T^{-3.01} \exp(-4932/T(\text{K}))$ and $3.4 \times 10^{24}T^{-2.77} \exp(-7196/T(\text{K}))$ at 101 Pa.

It is also interesting to investigate whether the reaction between benzyl and atomic hydrogen can lead to the formation

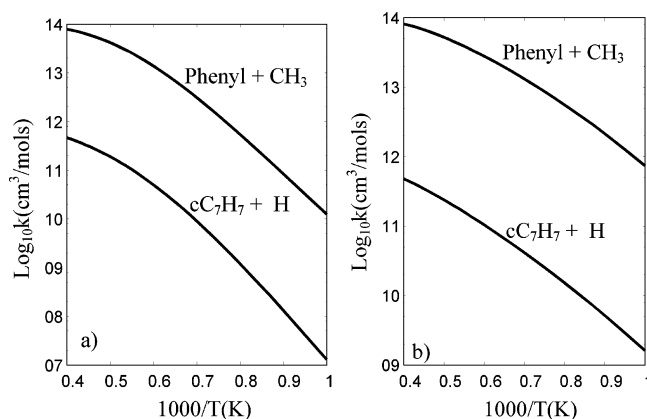


Figure 4. Results of bifrequency QRRK calculations performed for the reaction between H and benzyl at atmospheric (a) and reduced (101 Pa) (b) pressure.

of a substantial amount of cC₇H₇ following backward the reaction pathway outlined in Figure 2. The rate of production of phenyl and cC₇H₇ calculated at two different pressures are compared in Figure 4. The kinetic constants adopted for the bi-frequency QRRK calculations are the same reported in Table 1 with the addition of the high-pressure rate constant for the formation of toluene from benzyl and H of 2.010^{14} cm³/mol.s.

As it can be observed, the main product of the reaction is phenyl, which is produced more than 2 orders of magnitude faster than the C₇ species. Also, the absolute rate of production of benzyl at atmospheric pressure is about a factor of 2 smaller than that calculated by Klippenstein et al.¹⁸ using RRKM/master equation at low temperatures (900 K), while it is nearly the same at higher temperatures (2000 K). The same systematic underestimation of RRKM data was found at higher (10 bar) and lower (0.04 bar) pressures. This gives an indication of the level of approximation of the bifrequential QRRK approach here adopted with respect to a more sophisticated theory. In fact the difference between the two theories can entirely be attributed to the different level of description of the internal energy transfer process, since we used the same reaction rates for the formation and decomposition of the activated complex and the rate of formation of C₇ species is negligible with respect to that of stabilization of the excited adduct (toluene) and decomposition to phenyl and methyl. It can also be observed that, since the main product of the reaction is phenyl, this mechanism is unlikely to be a significant source of cC₇H₇ radicals in the gas phase.

The reaction rates calculated above can now be used to discuss which is the main reaction channel for cC₇H₇, after it is formed by the reaction between cC₅H₅ and C₂H₂. The competing reactions are the following





The relative importance of reactions R6, R7, and R8 is a function of the absolute concentrations of C_2H_2 and H and of the temperature at which the comparison is performed. For the sake of example, we refer to the temperature and composition measured in two different experiments reported in the literature. The first one refers to a fuel-rich acetylene/oxygen/argon laminar premixed flame ($\Phi = 2.4$, 5% argon, $v = 50$ cm/s, 20 Torr) which composition and temperature were experimentally measured by Westmoreland et al.³² As temperature and gas-phase composition are a function of the height above the burner, we referred to the values measured in correspondence to the peak temperature. The rate of reaction R7 was calculated as the sum of the rates of the reactions that lead to the production of benzyl and phenyl. The relative contribution of the three reaction channels to the overall cC_7H_7 reactivity was calculated as the rate of reaction R_i divided the sum of the rates of R6, R7, and R8. The computed relative importance was 0.92, 0.08, and 1.9×10^{-5} for R6, R7, and R8, respectively. The second experiments considered was the fuel-rich ethylene/oxygen/argon flame ($\Phi = 1.9$, 50% argon, $v = 62.5$ cm/s, 20 Torr) studied by Bhargava and Westmoreland et al.³³ The relative contributions of R6, R7, and R8 were 0.96, 0.04, and 3.1×10^{-6} . These results indicate that at high temperatures the major reaction pathway for cC_7H_7 , after being formed through the reaction between cC_5H_5 and C_2H_2 , is to decompose back to reactants. However, a significant percentage of cC_7H_7 , comprised between 4 and the 8%, can react with atomic hydrogen to form the stable benzyl radical. Though the ratio of converted cC_7H_7 might seem small, it must be pointed out that the ratio between the rate of the reaction of conversion of cC_7H_7 into a C6 cyclic species and that of decomposition to cC_5H_5 will increase with pressure, at parity of reactant mole fractions, as it is a bimolecular reaction in competition with a unimolecular decomposition reaction. For example, if the same calculation is performed at atmospheric pressure assuming that the hydrogen and acetylene mole fractions remain the same, then the rate of conversion into phenyl and benzyl becomes higher than that of dissociation to reactants.

On the basis of the above considerations, we can conclude that the mechanism we are proposing provides a kinetic pathway for the conversion of the cyclopentadienyl radical into a C6 species mediated by the formation of a seven-ringed species, cC_7H_7 . The feasibility of this reaction mechanism is confirmed by the fact that the cC_7H_7 formation rate we calculated is in agreement with experimental data measured at 1000 K, as discussed in our previous publication,¹⁰ and that cC_7H_7 is a chemical species sufficiently stable, because of the high number of resonance structures and internal symmetry, to survive at high temperatures for a time sufficient to react with atomic hydrogen and thus be converted efficiently to a more thermodynamically stable species such as the benzyl radical. On the other side, the reactivity trend discussed above clearly shows that, if cC_7H_7 is formed, it can decompose relatively fast to cyclopentadiene and acetylene. This reaction pathway provides therefore a mechanism by which C7 species can decompose to C5 species and acetylene, which has been in more occasions proposed in the literature as a possible decomposition channel for the benzyl radical. What remains to be explained to determine whether this decomposition channel is effective in flames is to find a fast conversion pathway between benzyl and cC_7H_7 . The reaction of cC_7H_7 and atomic hydrogen, however, seems not to be fast enough, given that its major product is the phenyl radical.

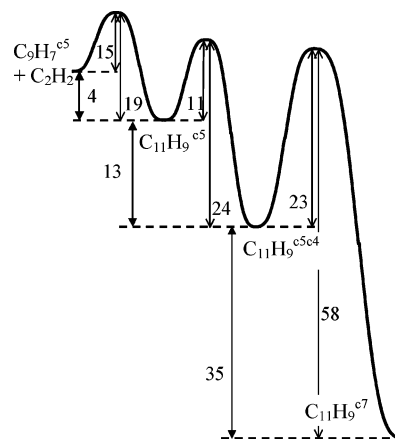


Figure 5. Activation energies and enthalpy changes for the $C_2H_2 + cC_9H_7$ reaction, whose kinetic pathway is reported in Scheme 5. All energies were calculated at the B3LYP/6-31+g(d,p) level and corrected with ZPE.

4. Reaction between C_2H_2 and the Indenyl Radical

To determine whether the mechanism of conversion of C5 into C7 and C6 species here proposed has the characteristic of generality and can be extended to species larger than cC_5H_5 and cC_7H_7 , we investigated the reactivity of C_2H_2 with the indenyl radical, which can be considered as the superior homologue of cC_5H_5 . The investigated reaction pathway is sketched in Scheme 5.

Because of the large number of atoms involved, the activation energies and reaction mechanism of the investigated pathway were calculated only at the B3LYP/6-31+g(d,p) level. The results are sketched in Figure 5, while the kinetic constants determined with conventional transition state theory are reported in Table 2. Similar to what was found for the $cC_5H_5 + C_2H_2$ reaction pathway, the addition of acetylene to the indenyl radical to form the activated $C_{11}H_9^{c5}$ adduct requires to overcome an activation energy of 15 kcal/mol, thus only 2 kcal/mol higher than that previously calculated. The $C_{11}H_9^{c5}$ adduct is stabilized by 4 kcal/mol with respect to the reactants, so that the dissociation reaction is very fast. However the $C_{11}H_9^{c5}$ adduct can react fast to form a tricyclic species, $C_{11}H_9^{c5c4}$ characterized by a C6, C5, and C4 ring, which is 17 kcal/mol more stable than the reactants and can further react to form a C6–C7 doubled-ringed species, the $C_{11}H_9^{c7}$ adduct, which is energetically stabilized with respect to reactants by a very high delocalization of the radical center. The $C_{11}H_9^{c7}$ adduct is in fact similar to the cC_7H_7 radical, though characterized by a smaller symmetry (C_{2v} with respect to D_{7h}).

The overall rate of the global reaction $C_9H_7^{c5} + C_2H_2 \rightarrow C_{11}H_9^{c7}$ was calculated between 1000 and 2500 K with the bifrequency QRRK theory using the same collisional stabilization parameters adopted to study the C_7H_8 PES. The rate of formation of the $C_{11}H_9^{c7}$ adduct is reported in Figure 6 at two different pressures as a function of temperature together with that of the intermediate adducts.

The $C_{11}H_9^{c7}$ adduct is the major product of the reaction between C_2H_2 and $C_9H_7^{c5}$, though the overall reaction rate is significantly slower than that of formation of the $C_{11}H_9^{c5}$ adduct. This indicates that, after being formed, a significant percentage of the energized $C_{11}H_9^{c5}$ complex dissociates to the reactants rather than react to form the $C_{11}H_9^{c7}$ adduct. Despite of this the overall rate of formation of $C_{11}H_9^{c7}$ is relatively fast, in particular considering the high concentration of the reactants usually observed in flames. It is also important to point out that the reaction pathway sketched in Scheme 5 is likely to be more

TABLE 2: Activation Energies and Kinetic Constants Calculated for the Reaction Mechanism That Follows the Addition of C₂H₂ to C₉H₇^{c5} and That Is Reported in Scheme 5^a

reaction	A_{forw}	α	$E_{a(\text{forw})}$	A_{back}	α	$E_{a(\text{back})}$
C ₉ H ₇ ^{c5} + C ₂ H ₂ → C ₁₁ H ₉ ^{c5}	3.5 × 10 ¹³	2.54	12.8	1.4 × 10 ¹⁴	0.08	21.15
C ₁₁ H ₉ ^{c5} → C ₁₁ H ₉ ^{c5c4}	1.5 × 10 ¹³	-0.15	11.9	4.4 × 10 ¹³	0.05	25.3
C ₁₁ H ₉ ^{c5c4} → C ₁₁ H ₉ ^{c7}	1.9 × 10 ¹³	0.09	24.4	7.5 × 10 ¹²	0.26	59.1

^a Kinetic parameters have been interpolated between 1000 and 2500 K and are reported as $k = AT^\alpha \exp(-E_a/RT)$ in units consistent with kcal, s, mol, and cm. Energies were calculated at the B3LYP/6-31+G(d,p) level and are corrected with ZPE.

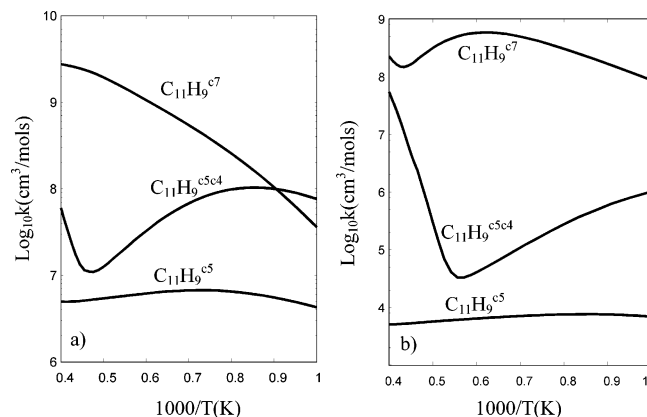
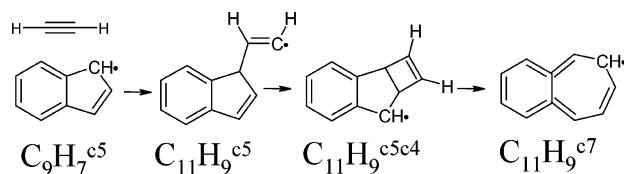


Figure 6. QRRK rate constants calculated for the reaction between C₂H₂ and C₉H₇^{c5} at the B3LYP/6-31+g(d,p) level at atmospheric (a) and reduced (101 Pa) (b) pressure.

SCHEME 5: Kinetic Mechanism Proposed To Describe the Reaction of the Indenyl Radical with Acetylene



complicated. For example acetylene might bind the indenyl radical also in positions different from those we chose to investigate, such as on the C6 cycle. Though these reactions are likely to have a smaller rate than that here investigated, because of the loss of resonance structures, the formed adducts might however isomerize to more stable structures, such as those here investigated, and thus increase the overall reaction rate.

Once formed the C₁₁H₉^{c7} radical species can follow a reaction pathway similar to that proposed for cC₇H₇. In particular we propose the mechanism sketched in Scheme 6 to describe its reaction with C₂H₂ to give fluorene.

Though this is only one of the several possible reaction mechanisms, fluorene is a thermodynamically stable PAH, and according to our calculations, the pathway that leads to its formation proceeds fast after overcoming the activation energy for the formation of the first activated complex, as is shown

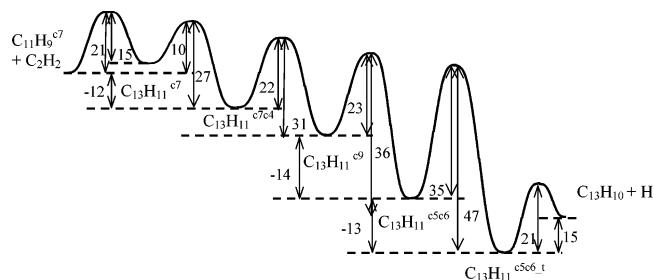
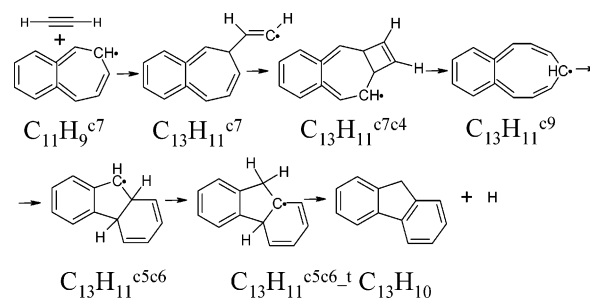


Figure 7. Activation energies and enthalpy changes for the H + C₁₁H₉^{c7} reaction, which kinetic pathway is reported in Scheme 6. All energies were calculated at the B3LYP/6-31+g(d,p) level and corrected with ZPE.

SCHEME 6: Kinetic Mechanism Proposed To Describe the Reaction of the C₁₁H₉^{c7} Radical with Acetylene



schematically in the PES diagram reported in Figure 7. The computed activation energies and kinetic parameters are reported in Table 3. The activation energy for the formation of the C₁₃H₁₁^{c7} adduct is 21 kcal/mol, thus 6 kcal/mol higher than that computed for the formation of the C₁₁H₉^{c5} adduct. This increase of activation energy is similar to that computed for the cyclopentadienyl reaction pathway previously investigated (7.5 kcal/mol) and is indicative of a decrease of reactivity of the C₇ cyclic species with respect to the C₅ species, which can reasonably be ascribed to the higher resonance stabilization of the C₇ ring. Also in this case it is possible that acetylene might bind C₁₁H₉^{c7} in positions different then those considered in Scheme 6. The explicit consideration of such reaction pathways might thus lead to an increase of the reactivity of C₁₁H₉^{c7}, which is however comprised between a factor of 1 and 5, given that C₁₁H₉^{c7} has C_{2v} symmetry and that the resonance radical centers are 11.

TABLE 3: Activation Energies and Kinetic Constants Calculated for the Reaction Mechanism That Follows the Addition of C₂H₂ to C₁₁H₉^{c7} ^a

reaction	A_{forw}	α	$E_{a(\text{forw})}$	A_{back}	α	$E_{a(\text{back})}$
C ₁₁ H ₉ ^{c7} + C ₂ H ₂ → C ₁₃ H ₁₁ ^{c7}	1.4 × 10 ⁵	2.07	19.4	6.9 × 10 ¹⁴	-0.111	17.5
C ₁₃ H ₁₁ ^{c7} → C ₁₃ H ₁₁ ^{c7c4}	2.6 × 10 ¹²	0.005	10.8	2.2 × 10 ¹³	0.045	28.5
C ₁₃ H ₁₁ ^{c7c4} → C ₁₃ H ₁₁ ^{c9}	1.8 × 10 ¹³	0.093	23.3	2.8 × 10 ¹³	-0.33	32.5
C ₁₃ H ₁₁ ^{c9} → C ₁₃ H ₁₁ ^{c5c6}	1.2 × 10 ¹⁰	0.46	21.8	1.1 × 10 ¹³	0.016	37.4
C ₁₃ H ₁₁ ^{c5c6} → C ₁₃ H ₁₁ ^{c5c6_t}	1.1 × 10 ¹²	0.26	35.7	3.3 × 10 ¹²	0.27	48.4
C ₁₃ H ₁₁ ^{c5c6_t} → C ₁₃ H ₁₀ + H	1.0 × 10 ¹²	0.48	22.4			

^a Kinetic parameters have been interpolated between 1000 and 2500 K and are reported as $k = AT^\alpha \exp(-E_a/RT)$ in units consistent with kcal, s, mol, and cm. Energies were calculated at the B3LYP/6-31+G(d,p) level and are corrected with ZPE.

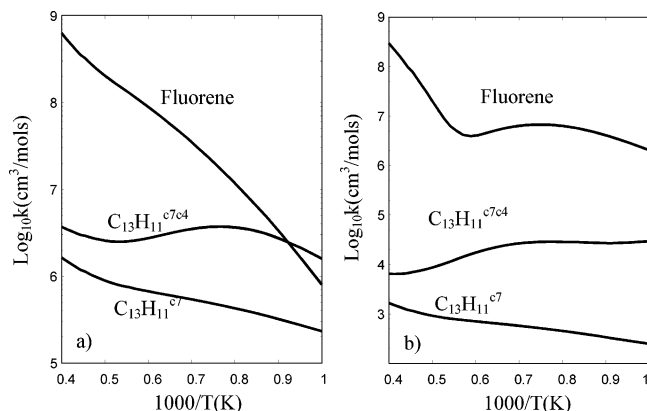


Figure 8. QRRK rate constants calculated for the reaction between C_2H_2 and $C_{11}H_9^{c7}$ at the B3LYP/6-31+g(d,p) level and atmospheric (a) and reduced pressure (101 Pa) (b).

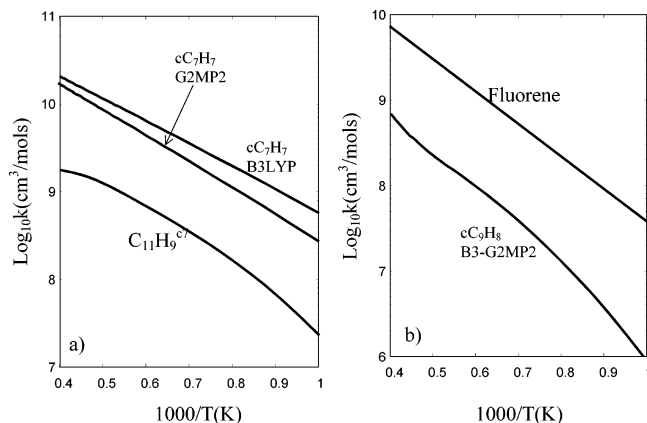


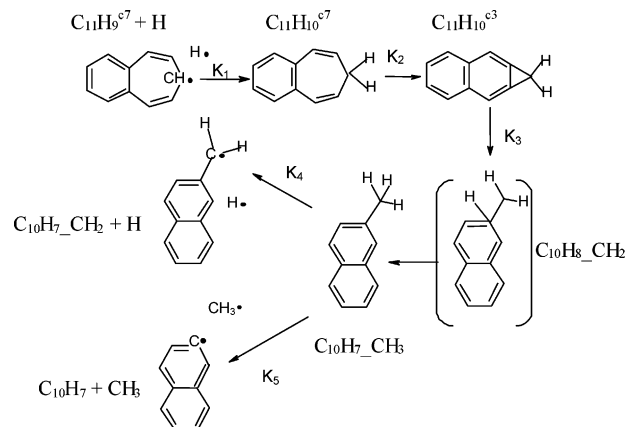
Figure 9. Comparison between QRRK rate constants calculated for (a) the reaction between C_2H_2 and C_9H_7c5 at the B3LYP/6-31+g(d,p) level and those determined previously for the reaction between C_2H_2 and cC_5H_5 at the B3LYP/6-31+g(d,p) and B3-G2MP2 levels and (b) the reaction between C_2H_2 and $C_{11}H_9^{c7}$ at the B3LYP/6-31+g(d,p) level and those determined previously for the reaction between C_2H_2 and cC_7H_7 at the B3-G2MP2 level.

Overall rates of the reaction between $C_{11}H_9^{c7}$ and C_2H_2 were computed with QRRK theory between 1000 and 2500 K for two different pressures and are reported in Figure 8. Collisional stabilization parameters used in the calculations are the same adopted for the cC_7H_8 PES.

As expected, fluorene is the main reaction product, though it is produced at a rate about an order of magnitude smaller than that computed for the formation of the $C_{11}H_9^{c7}$ radical. This can be ascribed to the activation energy that must be overcome to bind acetylene to the C7 cycle, which, as mentioned, is higher than that necessary to bind acetylene to the C5 ring.

In order to comment on the extensibility of the proposed reaction mechanism to similar or larger PAHs, it is interesting to compare the rate of formation of $C_{11}H_9^{c7}$ and fluorene with those previously determined for cC_7H_7 and indene, which are reported in Figure 9. Interestingly, it can be observed that calculated kinetic constants are not particularly sensible to the level of theory at which energies were computed. This is not determined by a similarity between the data computed at the two levels of theory but rather to the nature of the analyzed reacting systems. Overall reaction rates are in fact mostly determined by the rate of the entrance channel, which is the addition of C_2H_2 or H to a resonance radical and is only slightly activated. After the first activated complex is formed, it reacts fast to form the products. Thus the fact that the rate constant

SCHEME 7: Kinetic Mechanism Proposed for the Reaction between the $C_{11}H_9^{c7}$ Radical and Hydrogen



for the addition of C_2H_2 to the indenyl radical is about a factor of 10 smaller than that computed for the reaction between C_2H_2 and cC_5H_5 can be attributed almost entirely to the decrease of the pre-exponential factor of the reaction of addition of C_2H_2 to the radical. This is determined by the smaller rotational symmetry of $C_9H_7^{c5}$ with respect to that of cC_5H_5 , which accounts for a factor of 5, while the PESs of the two different reaction pathways are similar. The trend is similar also for the reaction between $C_{11}H_9^{c7}$ and C_2H_2 , whose rate is about an order of magnitude slower than that determined for the formation of indene from cC_7H_7 . It must however be pointed out that, as mentioned previously, the reaction pathways involving $C_9H_7^{c5}$ and $cC_{11}H_9^{c7}$ here investigated are based on the assumption that acetylene binds to the most reactive binding site of the two molecules. Alternative binding sites are however possible, and though the binding energy might be smaller with respect to the specific reaction pathways we choose to investigate, it might however increase the overall sticking coefficient of acetylene to these radicals and thus the overall reaction rate.

Finally we investigated the reactivity of $C_{11}H_9^{c7}$ with atomic hydrogen, which was previously shown to be the main reaction pathway for cC_7H_7 . The proposed reaction pathway, similar to that sketched in Scheme 3, is reported in Scheme 7. According to this mechanism, the addition of atomic hydrogen to $C_{11}H_9^{c7}$, which can be considered the homologue of heptatriene with an additional aromatic ring, can bring to the formation of 2-methyl naphthalene via the formation of $C_{11}H_{10}^{c3}$, the homologue of norcaradiene. Once the 2-methyl naphthalene is formed, dehydrogenation and pyrolysis steps can occur in parallel, leading to the formation of $C_{10}H_7-CH_2$, naphthenyl, hydrogen, and methyl radicals, that can consequently promote and continue the PAH growth. By consideration of Scheme 7 it is possible to underline that the mechanism proposed for the reaction of the $C_{11}H_9^{c7}$ radical with atomic hydrogen represents only one of the possible reaction pathways: in fact different $C_{11}H_{10}^{c7}$ isomers can be obtained depending on the C radical center to which atomic hydrogen binds. However, because of the complexity of the system, we decide to preliminarily study only the mechanism illustrated in Scheme 7.

Similarly to the transition from NCD to toluene, the localization of the transition state between 2-methyl naphthalene and $C_{11}H_{10}^{c3}$ was performed deeply analyzing the PES as a function of the three aforementioned characteristic reaction coordinates. The saddle point determining the transition state was found imposing that the force constants of all the reaction coordinates

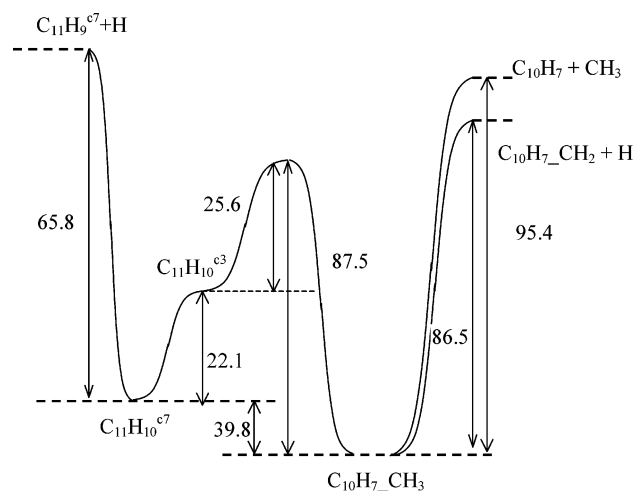


Figure 10. Activation energies and enthalpy changes for the H + $C_{11}H_9^{c7}$ reaction, whose kinetic pathway is reported in Scheme 7. All energies were calculated at the B3LYP/6-31+g(d,p) level and corrected with ZPE.

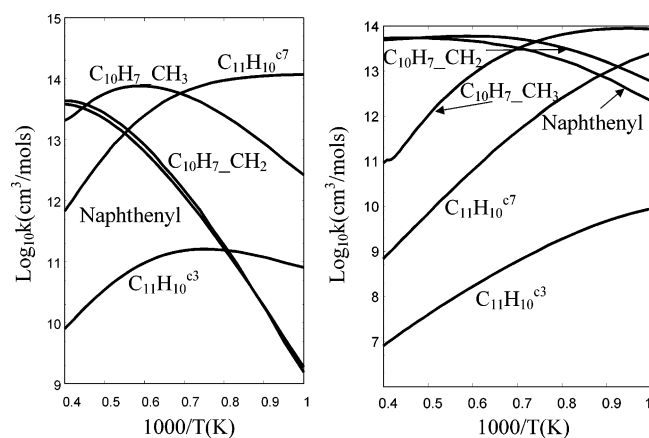


Figure 11. Results of bifrequency QRRK calculations performed at atmospheric (a) and reduced (101 Pa) (b) pressure for the reaction between H and $cC_{11}H_9$.

are smaller than 0.01 and was characterized through a frequency calculation by possessing a single imaginary vibrational frequency.

The rates for the $C_{11}H_{10}^{c7} \rightarrow C_{11}H_9^{c7} + H$ reaction and for the decomposition of 2-methyl naphthalene in the 2-naphthenyl and 2-naphthylmethyl radicals have been computed using VTST on PES calculated at the UB3LYP/6-31+g(d,p) level. The PES was determined varying between 2.0 and 4.0 Å at intervals of 0.1 Å the C–H and C–C distance for the hydrogen and methyl dissociation, respectively.

Activation energies and enthalpy changes, calculated at the B3LYP/6-31+g(d,p) level, are reported in Figure 10, while the kinetic constants are listed in Table 4. Overall rates of the reaction between $C_{11}H_9^{c7}$ and H to give the 2-naphthenyl and

2-naphthylmethyl radicals were computed with QRRK theory between 1000 and 2500 K for two different pressures and are reported in Figure 11. Collisional stabilization parameters used in the calculations are the same adopted for the cC_7H_8 PES.

The QRRK rates of conversion of $C_{11}H_9^{c7}$ into the 2-naphthenyl and 2-naphthylmethyl radicals are generally smaller than those computed for the conversion of cC_7H_7 into benzyl and phenyl. This can be ascribed almost entirely to the higher stability of the intermediate adducts determined by the larger number of vibrational degrees of freedom. Also in this case, however, it is true that the reaction pathway for collisional stabilized adducts such as $C_{11}H_{10}^{c7}$ is to isomerize to form methylnaphthalene and then dissociate to the 2-naphthenyl and 2-naphthylmethyl radicals rather than decompose to $C_{11}H_9^{c7}$. As the reaction with hydrogen is much faster than that with acetylene, it can be concluded that the two principal reaction pathways of $C_{11}H_9^{c7}$ at temperatures typical of combustion environments are either to dissociate to indenyl radical and acetylene or to react with atomic hydrogen and convert the C7 ring into a C6 ring.

These results suggest that the kinetic pathway we are proposing, namely, the increase in size of C5 cyclic species mediated by the formation of an intermediate C7 cyclic species, is likely to take place also for radical species larger than cyclopentadienyl radicals, provided that they contain a C5 ring stabilized by several resonance structures.³⁴

5. Conclusions

We have proposed a reaction mechanism by which C5 cyclic species, such as the cyclopentadienyl and the indenyl radical, can react with acetylene to form C7 cyclic species. The mechanism is relatively fast, as it requires overcoming small energetic barriers of 13–20 kcal/mol, and was found to be in agreement with experimental rate data for the reaction of the cyclopentadienyl radical with acetylene to form the cycloheptatrienyl radical. Once formed, the most likely reaction paths for the C7 cyclic species are either to decompose back to reactants or to react with atomic hydrogen and be converted to a C6 cyclic species, such as benzyl or phenyl if the reactant is the cycloheptatrienyl radical. The mechanisms here discussed provide therefore a new route for the conversion of C5 into C6 cyclic species mediated by the formation of C7 intermediate cyclic species. This mechanism is likely to be active both in the forward direction, which results in the increase in size of cyclic aromatics and provides therefore a possible route for the growth of PAH, and in the backward direction, which suggests a new and fast route for the decomposition of C7 species into C5 species.

Acknowledgment. We are grateful to S. Klippenstein for making his paper on the toluene decomposition available prior to publication.

TABLE 4: Activation Energies and Kinetic Constants Calculated for the Reaction Mechanism That Follows the Addition of H to $C_{11}H_9^{c7}$ ^a

reaction	A_{forw}	α	$E_{a(\text{forw})}$	A_{back}	α	$E_{a(\text{back})}$
$C_{11}H_9^{c7} + H \rightarrow C_{11}H_{10}^{c7}$	1.2×10^{14}	0	0	1.0×10^{18}	−0.85	68.9
$C_{11}H_{10}^{c7} \rightarrow C_{11}H_{10}^{c3}$	3.2×10^{12}	0.09	22.7	6.5×10^{12}	0	0
$C_{11}H_{10}^{c3} \rightarrow C_{10}H_7-CH_3$	2.8×10^{13}	0.34	27.6	1.1×10^{13}	−0.06	89.4
$C_{10}H_7-CH_3 \rightarrow C_{10}H_7-CH_2 + H$	6.6×10^{16}	−0.51	88.4	2.8×10^{14}	0	0
$C_{10}H_7-CH_3 \rightarrow C_{10}H_7 + CH_3$	3.4×10^{24}	−2.46	98.7	7.7×10^{12}	0	0

^a Kinetic parameters have been interpolated between 1000 and 2500 K and are reported as $k = AT^\alpha \exp(-E_a/RT)$ in units consistent with kcal, s, mol, and cm. Energies were calculated at the B3LYP/6-31+G(d,p) level and are corrected with ZPE.

Supporting Information Available: Atomic coordinates. This material is available free of charge via the Internet at <http://pubs.acs.org>.

References and Notes

- (1) Kunzli, N.; Kaiser, R.; Medina, S.; Studnicka, M.; Chanel, O.; Filliger, P.; Herry, M.; Horak, F.; Puybonnieux-Texier, V.; Quenel, P.; Schneider, J.; Seethaler, R.; Vergnaud, J. C.; Sommer, H. *Lancet* **2000**, *356*, 795.
- (2) Durant, J. L.; Busby, W. F.; Lafleur, A. L.; Penman, B. W.; Crespi, C. L. *Mutat. Res.-Genet. Toxicol.* **1996**, *371*, 123.
- (3) Siegmann, K.; Siegmann, H. C. *Molecular precursor of soot and quantification of the associated health risk*; Morán-Lopez, Ed.; Plenum Press: New York, 1998.
- (4) Richter, H.; Howard, J. B. *Prog. Energy Combust. Sci.* **2000**, *26*, 565.
- (5) Frenklach, M. *Phys. Chem. Chem. Phys.* **2002**, *4*, 2028.
- (6) Lindstedt, P.; Maurice, L.; Meyer, M. *Faraday Discuss.* **2001**, *119*, 409.
- (7) Frenklach, M.; Wang, H. *Proc. Combust. Inst.* **1991**, *23*, 1559.
- (8) Melius, C. F.; Miller, J. A.; Evleth, E. M. *Proc. Combust. Inst.* **1992**, *24*, 621.
- (9) Melius, C. F.; Colvin, M. E.; Marinov, N. M.; Pitz, W. J.; Senkan, S. M. *Proc. Combust. Inst.* **1996**, *26*, 685.
- (10) Fascella, S.; Cavallotti, C.; Rota, R.; Carra, S. *J. Phys. Chem. A* **2005**, *109*, 7546.
- (11) Knyazev, V. D.; Slagle, I. R. *J. Phys. Chem. B* **2002**, *106*, 10A.
- (12) Oehlschlaeger, M. A.; Davidson, D. F.; Hanson, R. K. *J. Phys. Chem. A* **2006**, *110*, 6649.
- (13) Frochtenicht, R.; Hippler, H.; Troe, J.; Toennies, J. P. *J. Photochem. Photobiol. A* **1994**, *80*, 33.
- (14) Jones, J.; Bacskay, G. B.; Mackie, J. C. *J. Phys. Chem. A* **1997**, *101*, 7105.
- (15) Schwell, M.; Dulieu, F.; Gee, C.; Jochims, H. W.; Chotin, J. L.; Baumgartel, H.; Leach, S. *Chem. Phys.* **2000**, *260*, 261.
- (16) Astholz, D. C.; Troe, J.; Wieters, W. *J. Chem. Phys.* **1979**, *70*, 1531.
- (17) Jarzecki, A. A.; Gajewski, J.; Davidson, E. R. *J. Am. Chem. Soc.* **1999**, *121*, 6928.
- (18) Klippenstein, S. J.; Harding, L. B.; Georgievskii, Y. *Proc. Combust. Inst.* **2007**, *31*, 221.
- (19) Marinov, N. M.; Pitz, W. J.; Westbrook, C. K.; Vincitore, A. M.; Castaldi, M. J.; Senkan, S. M.; Melius, C. F. *Comb. Flame* **1998**, *114*, 192.
- (20) Colket, M. B.; Seery, D. J. *Proc. Combust. Inst.* **1994**, *25*, 883.
- (21) Dean, A. M. *J. Phys. Chem.* **1985**, *89*, 4600.
- (22) Chang, A. Y.; Bozzelli, J. W.; Dean, A. M. *Z. Phys. Chem.* **2000**, *214*, 1533.
- (23) Troe, J. *J. Chem. Phys.* **1977**, *66*, 4745.
- (24) Troe, J. *J. Phys. Chem.* **1979**, *83*, 114.
- (25) Hippler, H.; Troe, J.; Wendelken, H. *J. Chem. Phys.* **1983**, *78*, 6709.
- (26) Curtiss, L. A.; Raghavachari, K.; Pople, J. A. *J. Chem. Phys.* **1995**, *103*, 4192.
- (27) Frisch, M. J.; Trucks, G. W.; Schlegel, H. B.; Scuseria, G. E.; Robb, M. A.; Cheeseman, J. R.; Montgomery, J. A., Jr.; Vreven, T.; Kudin, K. N.; Burant, J. C.; Millam, J. M.; Iyengar, S. S.; Tomasi, J.; Barone, V.; Mennucci, B.; Cossi, M.; Scalmani, G.; Rega, N.; Petersson, G. A.; Nakatsuji, H.; Hada, M.; Ehara, M.; Toyota, K.; Fukuda, R.; Hasegawa, J.; Ishida, M.; Nakajima, T.; Honda, Y.; Kitao, O.; Nakai, H.; Klene, M.; Li, X.; Knox, J. E.; Hratchian, H. P.; Cross, J. B.; Bakken, V.; Adamo, C.; Jaramillo, J.; Gomperts, R.; Stratmann, R. E.; Yazyev, O.; Austin, A. J.; Cammi, R.; Pomelli, C.; Ochterski, J. W.; Ayala, P. Y.; Morokuma, K.; Voth, G. A.; Salvador, P.; Dannenberg, J. J.; Zakrzewski, V. G.; Dapprich, S.; Daniels, A. D.; Strain, M. C.; Farkas, O.; Malick, D. K.; Rabuck, A. D.; Raghavachari, K.; Foresman, J. B.; Ortiz, J. V.; Cui, Q.; Baboul, A. G.; Clifford, S.; Cioslowski, J.; Stefanov, B. B.; Liu, G.; Liashenko, A.; Piskorz, P.; Komaromi, I.; Martin, R. L.; Fox, D. J.; Keith, T.; Al-Laham, M. A.; Peng, C. Y.; Nanayakkara, A.; Challacombe, M.; Gill, P. M. W.; Johnson, B.; Chen, W.; Wong, M. W.; Gonzalez, C.; Pople, J. A. *Gaussian 03*, revision C.01; Gaussian, Inc.: Pittsburgh, PA, 2003.
- (28) Tokmakov, I. V.; Moskaleva, L. V.; Lin, M. C. *Int. J. Chem. Kinetic.* **2004**, *36*, 139.
- (29) Kiefer, J. H.; Tranter, R. S.; Wang, H.; Wagner, A. F. *Int. J. Chem. Kinetic.* **2001**, *33*, 834.
- (30) Applegate, B. E.; Miller, T. A.; Barckholtz, T. A. *J. Chem. Phys.* **2001**, *114*, 4855.
- (31) Ikeda, E.; Tranter, R. S.; Kiefer, J. H.; Kern, R. D.; Singh, H. J.; Zhang, Q. *Proc. Combust. Inst.* **2000**, *28*, 1725.
- (32) Westmoreland, P. R.; Howard, J. B.; Longwell, J. P. *Proc. Combust. Inst.* **1986**, *21*, 773.
- (33) Bhargava, A.; Westmoreland, P. R. *Comb. Flame* **1998**, *113*, 333.
- (34) Frenklach, M.; Warnatz, J. *Combust. Sci. Technol.* **1987**, *51*, 265.